Available online at www.sciencedirect.com
ScienceDirect
Ceramics International 34 (2008) 45–49
CERAMICS INTERNATIONAL
www.elsevier.com/locate/ceramint

Nonhydrolytic sol–gel synthesis and dielectric properties of ultrafine-grained and homogenized $Ba_{0.70}Sr_{0.30}TiO_3$

Chaoliang Mao *, Xianlin Dong, Tao Zeng, Heng Chen, Fei Cao

Shanghai Institute of Ceramics, Chinese Academy of Sciences, 1295 Dingxi Road, Shanghai 200050, PR China

Received 28 March 2006; received in revised form 11 July 2006; accepted 20 August 2006
Available online 2 October 2006

Abstract

A simple process has been investigated to synthesize nanocrystalline $Ba_{0.70}Sr_{0.30}TiO_3$ (BST) powders via a nonhydrolytic sol–gel method by using barium acetate, strontium acetate, titanium tetrabutoxide, ethanol, acetic acid and acetylacetone as the starting materials. Thermogravimetry (TG) and differential thermal analysis (DTA) were used to examine the decomposition behaviour of the xerogel. The particle size of BST is close to 30 nm calculated by X-ray diffraction (XRD) and confirmed by transmission electron microscopy (TEM). Using these nanocrystalline BST powders, dense BST ceramics with ultrafine grains were obtained by spark plasma sintering (SPS). The grain size effect on the dielectric properties was studied. It was shown that as the grain size decreased, the transition temperature (T_c) and the dielectric constant decreased and the transition became diffuse.
© 2006 Elsevier Ltd and Techna Group S.r.l. All rights reserved.

Keywords: A. Sol–gel; $(Ba,Sr)TiO_3$; Nanocrystalline; Spark plasma sintering; Dielectric property

1. Introduction

Ferroelectric BST ($Ba_{1-x}Sr_xTiO_3$, $0 < x < 1$) is a kind of favorable electronic materials for its high dielectric constant and alterable Curie temperature with composition [1]. There is increasing interest for the use of BST in piezoelectric sensors, dynamic random access memories (DRAM), microwave phase shifters and uncooled infrared detectors [2,3] for its high dielectric, ferroelectric and pyroelectric properties. In order to attain the desired electrical characteristics, high chemical purity and uniform microstructure are the most important features for BST ceramics. Furthermore, the outstanding dielectric property observed on fine-grained BST ceramics has motivated the interest for the synthesis of the nanocrystalline BST. Conventional solid-state reaction is not suitable for preparing BST materials with high performance, as the calcining and sintering temperatures are too high. Compared to the conventional solid-state method, the synthesis of BST powder through chemical solution routes offers several advantages, such as high-purity, homogeneity and precise composition. There are a lot of chemical methods to prepare BST powders, such as co-precipitation, hydrothermal, polymeric precursor method and sol–gel process [4–7]. Stoichiometric deviation is the most crucial problem existing in the co-precipitation and hydrothermal process. Among others, sol–gel process is a favorable method for its low-temperature synthesis of BST nanopowders with high-purity and homogeneity. Conventional sol–gel process involves three primary steps: dissolution, hydrolysis and condensation [8]. However, the amount of water used during the initial two processes is extremely critical and uncontrollable. Inadequate and excess water may lead to the unhydrolyzation and precipitation in the solution, respectively. Furthermore, the quality of final product extremely depends on the amount of the water and pH [9]. All of these largely restrain the widespread applications of sol–gel method. Thus, in order to synthesize BST nanopowders simply and unrestrictedly, it is necessary and important to improve the conventional sol–gel method. The present paper describes an innovative and simple sol–gel process for the preparation of nanocrystalline BST powders at relatively low temperature without any water and out of the limit of pH. The nanosized nature of the BST powders was investigated by transmission electron microscopy (TEM). Fine and slight agglomerated powders are very useful and important to be sintered to

* Corresponding author. Tel.: +86 21 52412023; fax: +86 21 52413903.
E-mail address: maochaoliang@mail.sic.ac.cn (C. Mao).

0272-8842/$32.00 © 2006 Elsevier Ltd and Techna Group S.r.l. All rights reserved.
doi:10.1016/j.ceramint.2006.08.002

ultrafine-grained BST ceramics. Spark plasma sintering (SPS) of these powders were carried out to attain nano-grained and homogenized BST ceramics. The dielectric properties of the ceramics were discussed.

2. Experimental procedure

2.1. Materials

$Ba(CH_3COO)_2$, $Sr(CH_3COO)_2$ and $Ti(C_4H_9O)_4$ were used as starting materials to synthesize $Ba_{0.70}Sr_{0.30}TiO_3$ (BST) powders. Acetic acid and ethanol were selected as solvents for the acetates and alkoxide, respectively. Acetylacetone was used as an additive to stabilize the solution. Stoichiometric amounts of the individual solutions were thoroughly mixed in accordance with the $Ba_{0.70}Sr_{0.30}TiO_3$ composition. Acetylacetone (2 mol) per titanium ion was direct added to the transparent solution immersed in a basin with hot water (50–60 °C) and stirring. An orange sol could be obtained after 10 h. The sol was then put into an oven and dried for 12 h at 120 °C producing brown xerogel. The xerogel was fragile and could be crushed to coarse powders. The coarse powders will be hereinafter referred to as precursor. Heat treatment of the precursor at 800–900 °C in a muffle furnace resulted to nanocrystalline BST powder. A flow chart of the preparation of the nanocrystalline BST powder is shown in Fig. 1.

2.2. Characterization

The precursor thermogravimetric (TG) analysis and differential thermal analysis (DTA) were carried out under static air with a heating rate of 5 °C min^{-1} from room temperature to 1000 °C (NETZSCH STA 449C). IR spectra were recorded with a FT-IR spectrometer (Nicolet 7000-C) in the range 400–4000 cm^{-1} on as-pressed disks using KBr as the binding material. X-ray diffraction (XRD) with Cu Kα radiation (RAX-10) was carried out to examine the phase of the BST powders. The microstructure of the BST powders was investigated by transmission electron microscopy (JEM-2100F).

The nanocrystalline BST powders were then subsequently sintered in the form of disks by SPS. The powder was sieved using a 200-eye sieve and placed into a graphite die (15 mm in diameter) using a pressure of 50 MPa. The temperature was measured by using the thermoelectric couple inserting into the graphite die below 1000 °C. Densification was achieved when the temeperature increased to 980 °C for 2 min at the heating rate of 100 °C min^{-1}. The as-sintered pellets were annealed in oxygen at 800 °C for 2 h to eliminate the graphite. Densities of the sintered samples were measured according to the Archimedes principle. The morphology of the sintered compacts was studied using a scanning electron microscopy (JSM-6700F). Dielectric properties were measured by an impedance analyzer (HP4284A) at 0.1, 1, 10, 100 kHz using Ag as the electrode on both faces of the samples.

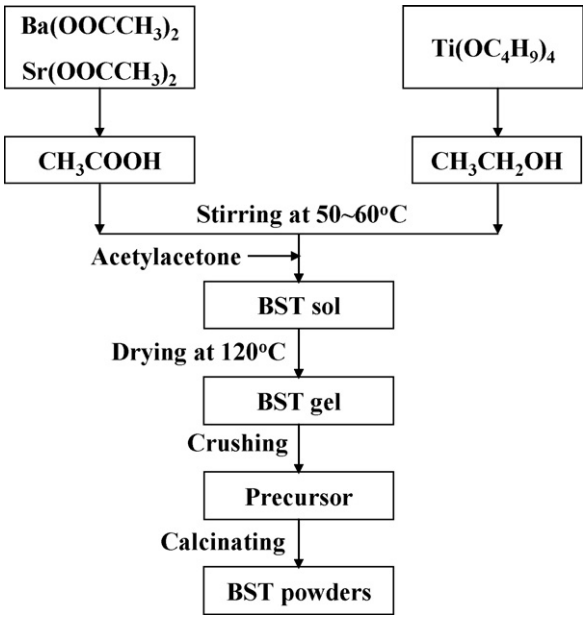

Fig. 1. Synthesis flowchart of nanocrystalline BST powders by the nonhydrolytic sol–gel method.

3. Results and discussion

Fig. 2 shows the IR spectrum of the precursor. Though it was very complex, the presence of broad bands at 3430 cm^{-1} (water stretching vibrations) [10], 2920 cm^{-1} (C–H stretching modes) [11], 1340 cm^{-1} (OH deformations of primary alcohols), 1050 cm^{-1} (C–O stretching vibration of primary alcohols) [11], 730 and 530 cm^{-1} (Ti–O stretching modes) [12] were evident. Particular interest is the fact that a set of two bands around 1500 cm^{-1}, 1430 and 1560 cm^{-1} were assigned to the stretching symmetric and antisymmetric vibrations in acetate ligands, respectively, acting as bidentate ligands with Ti according to the literatures [13,14]. This means that the butoxide ligands in $Ti(C_4H_9O)_4$ are exchanged by acetate ligands which coordinated with Ti in bidentate state. Kyoung et al. [14] suggested that as the formation of this coordination

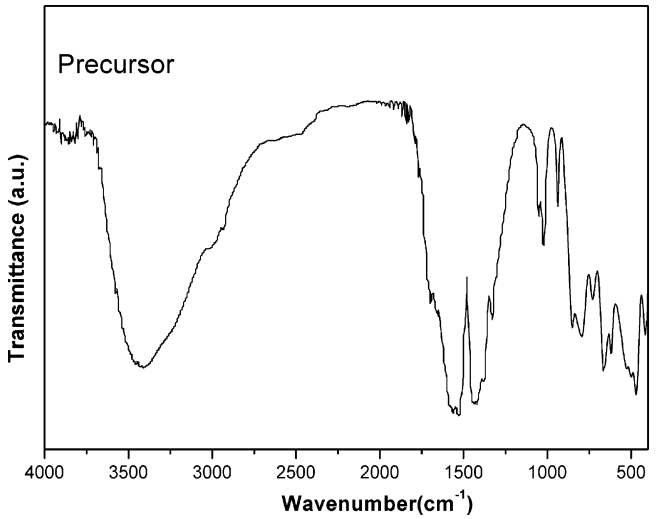

Fig. 2. FT-IR spectra of the precursor.

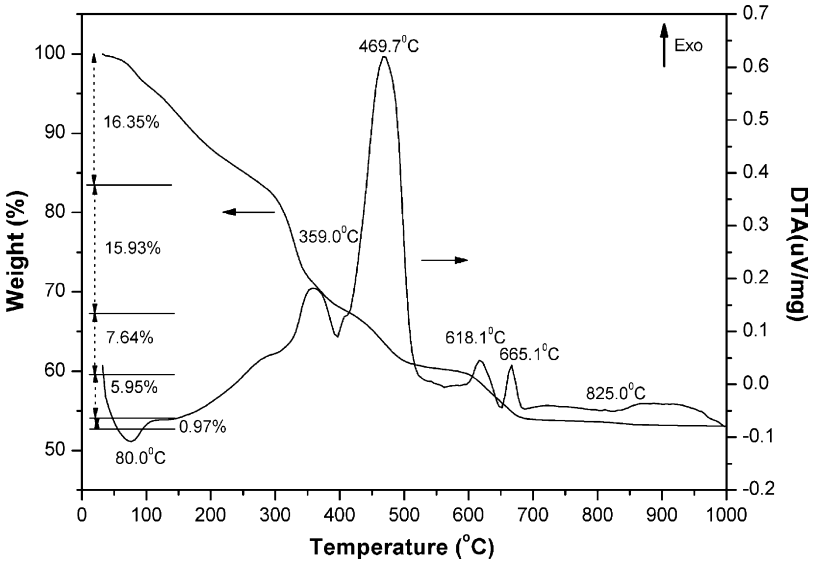

Fig. 3. TG and DTA curves of the precursor in static air from room temperature to 1000 °C.

mode, barium and strontium cations could have a strong interaction with titanium during the chelation. Further, work of the detailed formation mechanism of the precursor, in the absence of water, is in progress.

Fig. 3 shows the TG and DTA curves of the as-prepared precursor in static air. The TG trace indicates a five-step loss in the sample mass, corresponding to the evaporation of water adsorbed and acetic acid, the decomposition and combustion of the butyl alcohol, chelates and residues, the crystallization of BST powders at high temperature. During the first step, the weight loss was close to 16.35%, which can be attributed to the evaporation of water trapped at the surface of the precursor from atmosphere and a little amount of residual acetic acid. An endothermic peak near 80.0 °C was found in the DTA curve here. There was an exothermic peak around 359.0 °C corresponding to the combustion of the butyl alcohol derived from the exchange reaction between $Ti(C_4H_9O)_4$ and acetic acid. The weight loss during the third step was about 7.64% attributed to the decomposition and combustion of the chelates, accompanied by a sharp exothermic peak around 467.9 °C. As the temperature increased, two exothermic peaks near 618.1 and 665.1 °C appeared in DTA curve in the fourth step, corresponding to a loss in mass of 5.95% due to the combustion of organic residues. It should be noted that in the temperature range of 681.9–900 °C, there was little loss of mass about 0.97% during the last step, accompanied by a broad endothermic peak at 825.0 °C, which corresponded to the crystallization of BST via solid-state reaction between nanocrystalline carbonates and amorphous TiO_2. This can be confirmed by the XRD analysis. Fig. 4 shows the XRD patterns of BST powders prepared at different temperatures. It can be seen in Fig. 4(a) that there were two weak lines appearing at 24.18° and 34.40° corresponding to the residual carbonates phase, such as $BaCO_3$, $SrCO_3$ and $(Ba,Sr)CO_3$ [15]. At higher temperature, these peaks disappeared and a pure BST phase was obtained at 900 °C (refer to Fig. 4(b)). This indicates that as the temperature increased, the formation of BST via a solid-state reaction between nanocrystalline $(Ba,Sr)CO_3$ and amorphous TiO_2 happened.

The fine details of the pure BST powders and their morphology were investigated by TEM. Fig. 5 shows the TEM image of the particles obtained at 900 °C. Most of the powders were square in shape and slight agglomerated. The average particle diameter was found to be approximately 30 nm. This value was consistent with the result calculated by XRD (32 nm) using Scherrer's formula [16].

Fig. 6 shows the morphology of SPS sintered ceramics on the fracture surface of the sample. As the powders were well prepared, highly dense BST bodies (the relative density is about 98%) with ultrafine grains and uniform microstructure were obtained. The average grain size was about 170 nm and the grains were homogenized.

The temperature dependence of the dielectric constant (ε) of the 170 nm BST samples for several frequencies are

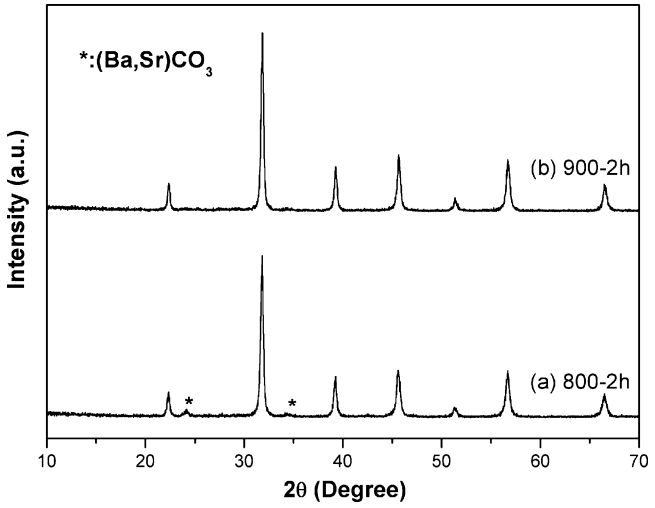

Fig. 4. XRD patterns of the BST powders synthesized at different temperatures: (a) 800 °C and (b) 900 °C.

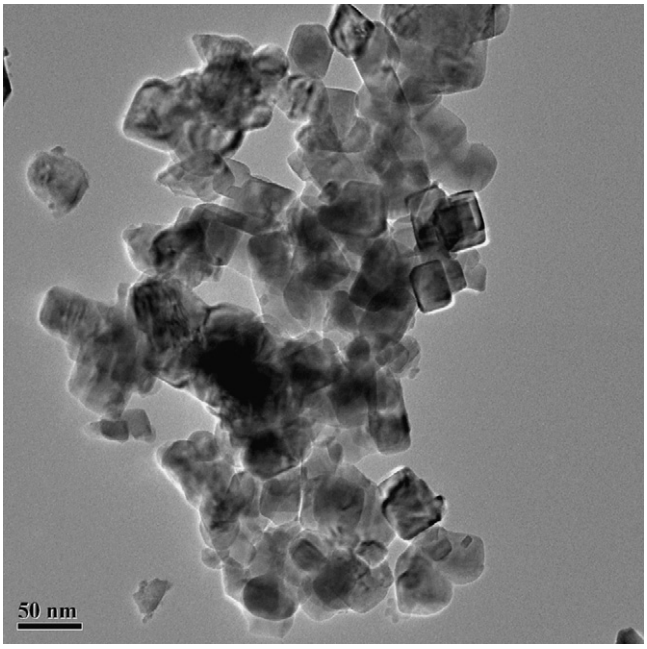

Fig. 5. TEM image of nanocrystalline BST powders obtained at 900 °C.

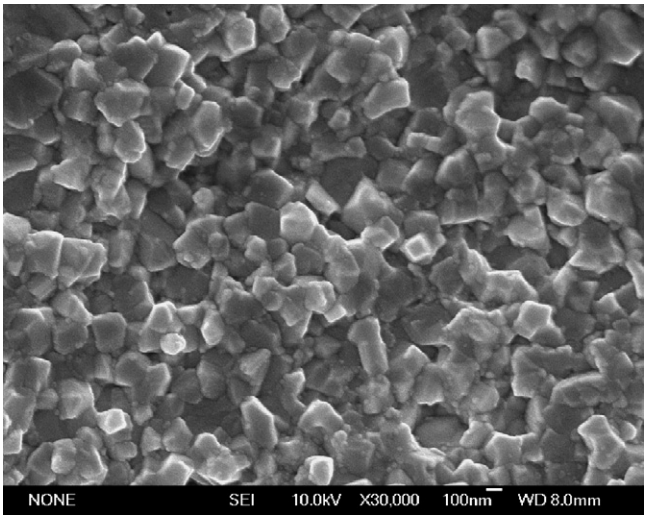

Fig. 6. SEM image of SPS sintered ceramics.

shown in Fig. 7(a) (inset is a zoom). For comparison, Fig. 7(b) shows the dielectric constant of $Ba_{0.70}Sr_{0.30}TiO_3$ ceramics with relatively coarse grains near 1 μm (the SEM image was not shown). Table 1 shows the dielectric constant of different grains under different frequencies at room temperature. It can be seen that both of the dielectric constants of the two samples decreased when the frequency increased. But the decrease of the dielectric constant of the ultrafine-grained sample was less than that of the coarsed-grained one. This implies the better stability of dielectric constant versus frequency of ulfrafine-grained sample. In Fig. 7 and Table 1, it should be noted that in the nano-grained BST ceramics, there was an evident diffuse phase transition and the transition temperature (T_c), tetragonal (ferroelectric) to cubic (paraelectric) transition temperature, decreased about 1.5 °C in the ultrafine-grained material. This could be attributed to the increased internal stress, which helped the ultrafine-grained material overcome the energy barrier of the transition [17]. Furthermore, the maximum value of ε was much smaller than that of the coarse-grained ceramics. This could be attributed to the total effects of the internal stress, grain boundary and domain wall contributions to the dielectric constant, which was similar to the result of $BaTiO_3$ [18].

Table 1
The dielectric constant of different grains under different frequencies at room temperature

Frequency (kHz)	Dielectric constant	
	1 μm, 25 °C	170 nm, 25 °C
0.1	10,364	2369
1	10,224	2324
10	10,040	2283
100	9,814	2240

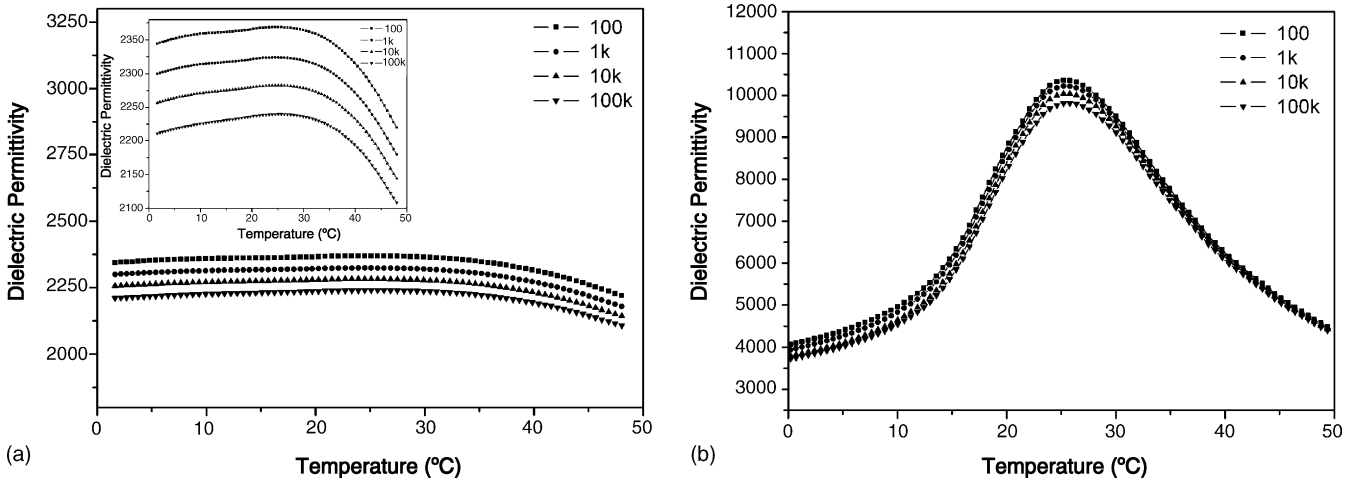

Fig. 7. Dielectric constant as a function of temperature at various frequencies for BST ceramics: (a) nano-grained (inset is a zoom) and (b) coarse-grained.

4. Conclusions

A modified nonhydrolytic sol–gel method has been successfully used to synthesize the nanocrystalline and slight agglomerated $Ba_{0.70}Sr_{0.30}TiO_3$ powders. Pure phase BST could be obtained at 900 °C. The particle size of the powder is about 30 nm. For the powders were well prepared, nanoscaled and homogenized BST ceramics with high density can be obtained by SPS. The average grain size of the ceramics was about 170 nm. Compared to the relatively coarse-grained material, the ulfrafine-grained sample exhibits the better stability of dielectric constant versus frequency. Dielectric data show a broad phase transition and decreased value of ε due to the nanoscaled grains. This low-temperature synthetic route, eliminating the disadvantages of the water and requiring only simple raw materials, respectively, will offer a new strategy for preparing nanoscaled powders and homogenized ceramics in many electronic applications.

References

[1] K. Bethe, F. Welz, Preparation and properties of (Ba,Sr)TiO_3 single crystals, Mater. Res. Bull. 6 (1971) 209–217.
[2] J.Y. Wang, X. Yao, L.Y. Zhang, Preparation and dielectric properties of barium strontium titanate glass-ceramics sintered from sol–gel-derived powders, Ceram. Int. 30 (2004) 1749–1752.
[3] H.M. Jang, Y.H. Jun, (Ba,Sr)TiO_3 system under dc-bias field. II: induced and intrinsic pyroelectric coefficients and figures-of-merit, Ferroelectrics 193 (1997) 125–140.
[4] F. Schrey, Effect of pH on the chemical preparation of barium–strontium titanate, J. Am. Ceram. Soc. 48 (1965) 401–405.
[5] R.K. Roeder, E.B. Slamovich, Stoichiometry control and phase selection in hydrothermally derives $Ba_xSr_{1-x}TiO_3$ powders, J. Am. Ceram. Soc. 82 (1999) 1665–1676.
[6] R.N. Das, P. Pramanik, Chemical synthesis of nanocrystalline $BaTiO_3$ and $Ba_{1-x}Sr_xTi_{1-y}Zr_yO_3$ [(i) $x = 0.03$, $y = 0$, (ii) $x = 0$, $y = 0.03$] ceramics, Nanotechnology 15 (2004) 279–282.
[7] P.K. Sharma, V.V. Varadan, V.K. Varadan, Porous behavior and dielectric properties of barium strontium titanate synthesized by sol–gel method in the presence of triethanolamine, Chem. Mater. 12 (2000) 2590–2596.
[8] R.C. Mehrotra, Chemistry, spectroscopy and applications of sol–gel-glasses, monograph series, Struct. Bond. 77 (1992) 153–157.
[9] C.J. Brinker, G.W. Scherer, Sol–gel Science: The Physics and Chemistry of Sol–gel Processing, Academic, Boston, 1990.
[10] J.D. Tsay, T.T. Fang, T.A. Gubiotti, J.Y. Ying, Evolution of the formation of barium titanate in the citrate process: the effect of the pH and the molar ratio of barium ion and citric acid, J. Mater. Sci. 33 (1998) 3721–3727.
[11] L.J. Bellamy, The Infra-red Spectra of Complex Molecules, Methuen & Co Ltd., London, 1958.
[12] P. Durán, F. Capel, D. Gutierrez, J. Tartaj, M.A. Bañares, C. Moure, Metal citrate polymerized complex thermal decomposition leading to the synthesis of $BaTiO_3$: effects of the precursor structure on the $BaTiO_3$ formation mechanism, J. Mater. Chem. 11 (2001) 1828–1836.
[13] S. Doeuff, M. Henry, C. Sanchez, J. Livage, Hydrolysis of titanium alkoxides: modification of the molecular precursor by acetic acid, J. Non-Cryst. Solids 89 (1987) 206–216.
[14] S.K. Kyoung, W.S. Ill, C.J. Han, The preparation of $BaTiO_3$ and $Ba_{0.65}Sr_{0.35}TiO_3$ powders from complex acetate precursors, J. Korean Phys. Soc. 32 (1998) 1227–1230.
[15] H.Y. Tian, J.Q. Qi, Y. Wang, J. Wang, H.L.W. Chan, C.L. Choy, Core-shell structure of nanoscaled $Ba_{0.5}Sr_{0.5}TiO_3$ self-wrapped by MgO derived from a direct solution synthesis at room temperature, Nanotechnology 16 (2005) 47–52.
[16] M.P. Klug, L.E. Alexander, X-ray Diffraction Procedure for Polycrystalline and Amorphous Materials, Wiley, New York, 1974.
[17] B.W. Lee, K.H. Auh, Effect of grain size and mechanical processing on the dielectric properties of $BaTiO_3$, J. Mater. Res. 10 (1995) 1418–1423.
[18] A.S. Shaikh, R.W. Vest, G.M. Vest, Dielectric properties of ultrafine grained $BaTiO_3$, IEEE Trans. Ultrason. Ferroelect. Freq. Contr. 45 (1998) 1444–1452.